

Mechanical characterisation of adobe samples from the state of Morelos, Mexico

Paper (reviewed on 24th of April 2023) – 4995 words, 10 tables, 9 figures.

Author 1

- Rafael Ramírez Eudave, MSc
- ISISE – Institute for Sustainability and Innovation in Structural Engineering, University of Minho, School of Engineering, Civil Engineering Department, Azurém Campus, 4800-058 Guimarães, Portugal. Email: r.92@outlook.es
- <https://orcid.org/0000-0003-0733-6685>

Author 2

- Tiago Miguel Ferreira, PhD
- College of Arts, Technology and Environment, University of the West of England, Bristol, UK. Email: Tiago.Ferreira@uwe.ac.uk.
- <https://orcid.org/0000-0001-6454-7927>

Author 3

- Paulo B. Lourenço, PhD
- ISISE – Institute for Sustainability and Innovation in Structural Engineering, University of Minho, School of Engineering, Civil Engineering Department, Azurém Campus, 4800-058 Guimarães, Portugal. Email: pbl@civil.uminho.pt
- <https://orcid.org/0000-0001-8459-0199>

Author 4

- Fernando Peña, PhD
- Instituto de Ingeniería, Universidad Nacional Autónoma de México, Mexico City, Mexico. Email: fpem@pumas.iingen.unam.mx.

Author 5

- Marcos Chávez, PhD
- Instituto de Ingeniería, Universidad Nacional Autónoma de México, Mexico City, Mexico. Email: mchavezc@pumas.iingen.unam.mx.

Corresponding Author: Rafael Ramírez Eudave, r.92@outlook.es

Abstract

Adobe properties are highly dependent on the local soil composition and can vary significantly depending on fabrication techniques, configurations and state of conservation. The effect of the 2017 Earthquakes in Mexico relaunched the discussion regarding the adequacy and safety of adobe-based constructions – a debate that involves many economic, cultural and social facets related to the vernacular expressions and ways of life, long-time sustainability and risk management. In an effort to contribute to this, the present article includes and discusses a series of experiments performed in typologically representative adobe constructions in the municipality of Tepoztlán (State of Morelos, Mexico). A campaign of ultrasonic pulse velocity tests was conducted in thirteen historical buildings with the objective of assessing the variability of the adobe material present in those buildings. Some adobe units were then collected and tested in the laboratory to assess their compressive strength and stress/strain behaviour. From these two sets of experiments, it was possible to obtain valuable insights into the mechanical properties of the adobe that constitute the characteristic housing typology in the region.

Keywords: Earthquakes, In situ testing, Safety and hazards. Clays, Compressive Strength.

List of notations.

M_w	is the seismic intensity in EMS-98 Scale
v_p	is the velocity of propagation of a longitudinal elastic p-wave
ρ	is the density of the tested material
E_D	is the dynamic elastic modulus
ν	is the Poisson's ratio
E	is the static elastic modulus
ε_x	is the strain in the XX direction
ε_y	is the strain in the YY direction

1. Introduction

A critical aspect of risk mitigation and management lies in assessing the ability of the existing infrastructures and buildings to cope with extreme events, such as earthquakes. This awareness regarding the vulnerability of existing constructions is associated with the expectancy of damages in post-seismic scenarios (Gavarini, 2001). Identifying vulnerable structures at the urban scale presents several challenges, including variability in structural typologies and the ongoing processes of modification and changes in use that many of these buildings have undergone over time. This is especially complex when dealing with historical constructions, where singularities prevent generalisations even within typologically similar constructions.

In September 2017, two strong earthquakes hit Mexican territory. The first one (7th September), later known as the “Tehuantepec Earthquake”, had an intensity of $M_w=8.2$ and provoked extensive damages in the southern states of the country. A second event, on 19th September (later named “Puebla-Morelos Earthquake”), had an intensity of $M_w=7.1$ and impacted the centre and south regions of Mexico. More than 23,000 buildings in the state of Morelos alone (a state with ca. 1.972 million hab. located south of Mexico City) were damaged. From these, some 7,300 were reported as destroyed (Archundia-Aranda, 2020). Historical constructions represented a significant proportion of the damaged structures (Godínez-Domínguez *et al.*, 2021) and within this group, vernacular adobe buildings were commonly perceived as particularly vulnerable. This is particularly meaningful considering that adobe structures represent more than 20% of housing units in certain municipalities in the State of Morelos (Sánchez Calvillo, Alonso Guzmán and López Núñez, 2021), particularly in the rural areas of the state. These examples of vernacular constructions represent a material response to the material availability and climatic conditions of this region (Rojas, Ferrer and S, 2009).

During the post-event disaster management, there was a heated debate centred on discussing the safety levels that adobe-based structures offer towards seismic actions (Chmutina, Jigyasu and Okubo, 2020). This debate often pitted the risk perception of the inhabitants, based on the empirical observations (i.e., the extensive damages on adobe structures), against the cultural loss represented by the demolition of these structures, which, according to several experts in this field, could be

avoided through the implementation of well-reasoned structural repair and retrofitting interventions (Guerrero Baca and Soria López, 2018). According to the Historic Urban Landscape principles (UNESCO, 2016), the loss of these assets represents irreparable damage to the cultural heritage of cities.

Taking care of and preserving cultural heritage is an ongoing activity that can be incorporated into large-scale initiatives such as risk mitigation actions outlined in the Chart of the Sendai Framework for Disaster Risk Reduction 2015-2030 (United Nations, 2015). However, the practice of risk mitigation policies depends on understanding risk and, therefore, characterising vulnerabilities and the current state of cultural assets. A critical step in performing these assessments is estimating the mechanical properties of materials and structures.

This study presents an experimental program conducted on historical buildings in the municipality of Tepoztlán, state of Morelos, Mexico, intending to provide insight into the mechanical properties of the adobe used in this region. The first stage of this experimental work involved conducting ultrasonic pulse velocity tests on the structural elements (columns and walls) of thirteen historical buildings with the primary objective of understanding material variability. Adobe samples were also collected and tested in the laboratory of the Institute of Engineering of the National Autonomous University of Mexico, where compressive tests were conducted to observe strain/stress behaviour.

It is worth noting that the municipality of Tepoztlán was chosen as a case study in the context of a larger campaign to assess vulnerability through a series of parametric descriptions. The municipality is home to a significant number of vernacular houses with a regular typology, creating a mixed cultural and natural environment that supports tourism and promotes the preservation of architectonic heritage (Uhnák, 2018).

2. Materials and testing protocols

The experiments presented and discussed in this paper were conducted on buildings (or on adobe material collected from buildings) considered historical monuments by Mexican law, which stipulates that any construction built before 1900 is automatically recognised as historic. These

buildings are therefore listed in the Mexican National Catalogue of Historical Constructions (Ramírez Eudave and Ferreira, 2021).

2.1 Ultrasonic pulse propagation velocity

A series of tests to determine the velocity of ultrasonic wave propagation were performed in situ, totalling 117 successful measurements on 39 different samples (i.e., each sample was measured three times to obtain a mean value) in 13 different buildings. The possibility of performing direct and indirect tests was heavily constrained by the facilities provided by the owners of the buildings. Despite the ideal procedure being to test both internal and external materials (given the sensitivity of adobe towards weathering), in most cases, owners only allowed the team to work from the exterior of the buildings (Figure 1), mainly due to public safety concerns. The number of measurements of each type is presented in Table 1. The nomenclature adopted expresses the type of measurement and the number of mortar joints traversed by the elastic wave.



Figure 1. Examples of direct ultrasonic wave propagation measurements in a column (A) and a wall (B) and an indirect measurement in the external face of a façade wall (C)

Table 1. Summary of type and number of measurements.

Type	Samples	Description
Direct 0	12	Opposite sides of the wall, measuring a simple adobe unit.
Direct 1	1	Opposite sides of the wall passing through one mortar joints

Direct 2	2	Opposite sides of the wall passing through two mortar joints
Indirect 0	19	From the same side of the adobe unit
Indirect 1	3	From the same side of the wall passing through one mortar joint.
Indirect 2	2	From the same side of the wall passing through two mortar joints
Total	39	

The equipment used for this purpose was a Pundit Array 250 device equipped with standard kHz transducers for testing the pulse velocity of P-waves. The pulse voltage was set for all measurements at 150 V, and the probe gain was kept at 500x. The test protocol involved cleaning the surface of the specimens with a soft brush, as well as cleaning and covering the sensors with a contacting gel to improve the propagation of the waves between the transducers to the specimens. When a measurement was successful (i.e., the ultrasonic waves were effectively transmitted), two additional measurements were taken at the same location. All non-repeatable observations were excluded.

2.2 Mechanical characterisation of adobe units

As mentioned before, these experiments were designed to determine the compressive strength, modulus of elasticity and Poisson ratio of the building material of most vernacular constructions in the studied region. All the tests were conducted in the Structures Laboratory of the Institute of Engineering of the National Autonomous University of Mexico using a universal testing machine. The experimental program consisted of two sets of experiments:

a) Preliminary unconfined compressive strength tests on small samples (referred to as A, B, and C in Table 2) to determine an indicative failure strength of the material and calibrate suitable load cycles for the remaining samples;

b) Unconfined compressive strength tests on complete adobe blocks (referred to as I, II, III and IV in Table 2) adopting three cycles of loading and unloading below the indicative elastic limits of compressive strength. Strains in the blocks were monitored using an OptoTrack system (details can be found in Subsection 2.2.3).

2.2.1 Materials

It is convenient to emphasise that the obtention of materials from historical constructions is subjected to several challenges. The obtention of the materials herein presented is the result of large-scale field campaigns in which the vast majority of inhabitants refused the material collection for testing purposes. The negative reaction of the buildings' users was commonly associated with public safety concerns and the feeling of not getting any benefit from donating materials for the experimental campaign. Nevertheless, a set of samples was generously donated.

The samples tested in this experimental campaign were collected in the municipality of Tepoztlán during a fieldwork action on 18th August 2022. A set of four pieces were donated by the owner of a building listed in the Mexican National Catalogue of Historical Monuments (0071) as a historical construction. According to the donator, these adobe units (Figure 2) were recovered from partially collapsed walls on their property, which was allegedly built at the end of the 19th century.



Figure 2. Pile of blocks from which the samples for the experiments in this study were obtained. Note that these pieces were stored in outdoor conditions.

The pieces that appeared to be in the best condition were selected from those offered. The largest piece, substantially bigger than the rest, was divided into pieces (samples A, B and C) in order to perform the preliminary calibration tests. The remaining samples (I, II, III and IV) were kept in their original conditions. The description of all the samples is summarised in Table 2.

Table 2. Summary of the samples

Key	Length [m]	Thickness [m]	Height [m]	Mass [kg]	Density [$\frac{\text{kg}}{\text{m}^3}$]
A	0.14	0.13	0.11	2.43	1258.74
B	0.13	0.11	0.11	1.74	1262.59
C	0.17	0.11	0.12	2.51	1259.80
I	0.28	0.10	0.37	13.35	1356.43
II	0.18	0.10	0.27	5.87	1230.61
III	0.18	0.10	0.27	6.62	1433.83
IV	0.20	0.10	0.27	6.60	1277.21

The value of the density of these specimens (with a mean of 1333.56 kg/m³) is lower than most of the typical values found in the literature for Mexican adobe. Some studies report density values in the order of 1800 kg/m³ (Ruiz Sibaja and Vidal Sánchez, 2015; Juarez, Caballero and Morales, 2016), while some recommendations accept values of about 1600 (CEMEX, 2013) or even 1500 kg/m³ (Tyrakowski, 2013). The experimental campaign of Catalán Quiroz *et al.* (2019) reported densities of ca. 1370 kg/m³ which is close to the values found during this work. Given that the composition of adobe is very dependent on the local soil properties and the aggregates (if any), these relatively low densities may be related to internal voids, external disaggregation or a relatively high presence of vegetal fibres.

According to residents, these adobes were originally made from a mixture of local soil, collected near the construction site, and a proportion of horse manure, which was then compressed in formworks and left to dry in the sun. The inclusion of manure in this composition is significant because it adds vegetable fibres that were supposed to enhance the stability of the pieces. Experimental evidence of the positive impact of this retrofitting has been reported in several studies, such as those of Ruiz Serrano (2019) and Jerónimo-Vargas *et al.* (2022). When inquired about the traditional dynamics for producing adobe housing, most of the inhabitants agreed on describing the adobe

127 manufacture as a craft with a reduced number of experts that used to cover the needs of the entire
128 settlement. The sizes, composition and processes are quite homogeneous given the reduced number
129 of specialists and the father-to-son transmission. Even today, adobe fabrication faces the lack of local
130 regulations and relies on traditional know-how.

131 2.2.2 Preliminary compressive tests

132 48h before testing, all the adobe samples were prepared by adding a layer of gypsum to create
133 a more regular contact surface between the adobe units and the machine (Figure 3). This ensured
134 the elimination of any possible stress concentration points and ensured that the specimens were
135 tested for pure compressive strength.



136
137 Figure 3. Set of samples after preparation with gypsum.

138 The first set of tests (on specimens A, B and C) was conducted following a load-based control
139 protocol at a constant rate of 5 kN/min until reaching visible failure. The maximum load for these
140 specimens was 8.46, 5.90 and 11.68 kN, respectively. Based on these observations, the maximum
141 failure stress was in the range of 0.41 to 0.67 MPa. Therefore, it was decided to adopt controlled load
142 cycles of 2.6 kN for testing the subsequent samples before reaching failure.

143 2.2.3 Unconfined compressive strength tests with strain measurement

The conduction of the unconfined compressive strength was aided by two OptoTrack Certus HD Position Sensor devices and infrared LED arrays to measure strain on the surface of the specimens in the two main directions on both sides of each specimen. The sensor was composed of three cameras that tracked the displacements of a set of infrared LEDs in the X, Y and Z axis with a resolution of 0.01 mm. These devices can be set to follow multiple surfaces using a common spatial coordinate reference (Figure 4).



Figure 4. View of the OptoTrack devices.

Four LEDs were installed in each face of the specimens, arranged in a cross concentric with the geometrical centre of the specimen. This configuration provided two extensometers in the XX and YY axes, as shown in Figure 5. The original length of the extensometers for Specimen I was approximately 200 mm, while those for Specimens II, III, and IV were 150 mm. The initial length of the arrays, as measured by the cameras, is reported in Table 3. During the experiment, the use of both devices allowed for real-time measurements of both faces of the specimens at a frequency of 0.1s. This sampling rate was selected to improve synchronisation with the outputs of the universal testing machine.

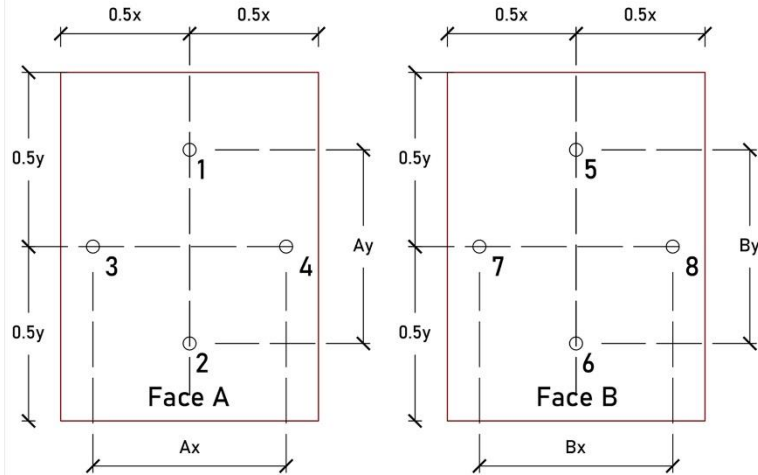


Figure 5. Schematisation of the infrared LEDs array.

Table 3. Summary of extensometers and original length according to the OptoTrack measurements.

Specimen	Ax [mm]	Ay [mm]	Bx [mm]	By [mm]
I	200.77	201.67	204.34	198.62
II	150.18	146.28	150.43	148.98
III	148.81	144.66	149.40	145.57
IV	145.15	148.56	148.21	150.62

These specimens were tested in two stages. An initial pre-charge of 0.1 kN was applied to ensure good contact between the machine's plates and the specimen. Three load cycles were then performed, reaching 2.6 kN (with a load-controlled rate of 5kN/min) and releasing the load until reaching 0.1 kN each time. The fourth load ramp was continued until the failure of the specimen. The failure threshold was reached when the compressive strength fell below 60%.

3. Results and discussion

3.1 Ultrasonic tests

As can be seen in Table 4, the results of the ultrasonic pulse velocity tests (also reported in Appendix 1) showed a high level of variability, with velocities ranging from 393 to 1,238 m/s. The distribution of the velocities plotted in the histograms given in leads to excluding the hypothesis of normality for both direct and indirect tests. The hypothesis of a "monolithic" behaviour of adobe walls,

in which the material used in the joints was assumed to be similar to that of the blocks, seems to be, therefore, not supported by the data.

Table 4. Summary of descriptive statistics

Type	Samples	Mean velocity [m/s]	Mean velocity [m/s]	Standard deviation	Coefficient of Variation
Direct 0	12	703.96	603.66	258.55	0.37
Direct 1	1	493.33	-	-	-
Direct 2	2	437.00	437.00	10.84	0.02
Indirect 0	19	507.01	480.66	90.60	0.18
Indirect 1	3	516.22	488.00	88.76	0.17
Indirect 2	2	394.50	394.50	1.65	0.00

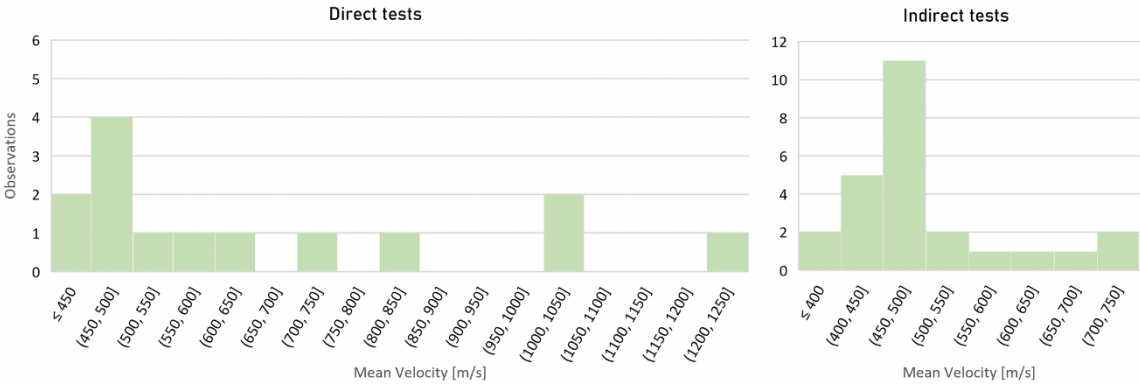


Figure 6. Histogram for direct and indirect tests.

The first interpretation of these results suggests a high level of variability that makes it difficult to identify a typical range for analysis, particularly due to the discontinuity between the median and higher values. However, this inconclusiveness can be contextualised, and a different interpretation is possible. Three direct tests showed significantly higher velocities than the others (1,005, 1,009 and 1,238 m/s), though a visual inspection of these elements did not reveal any significant difference. Potential explanations for this difference include an atypical composition of adobe (e.g., with more rigid elements, such as stones or sand) or the presence of strengthening elements; bars, for example.

The addition of slender canes (e.g., reed canes) was referred to by some inhabitants even if their presence was not witnessed during the field campaigns.

The three above-mentioned values, which significantly increase the samples' overall variability, were all obtained from the same structure. Having this in mind and considering that 12 constructions (rather than 13) still constitute a significant sample of buildings, an alternative interpretation was performed by assuming that these values are outliers and excluding them from the analysis. The result of that approach is a considerably more uniform set of results, as can be observed in Figure 7. However, the Shapiro-Wilk test for normality still showed that neither the results of direct ($W(12) = 0.8444$, $p=0.040$) nor those of the indirect tests (and $W(24) = 0.834$, $p = 0.001$) are normality distributed.

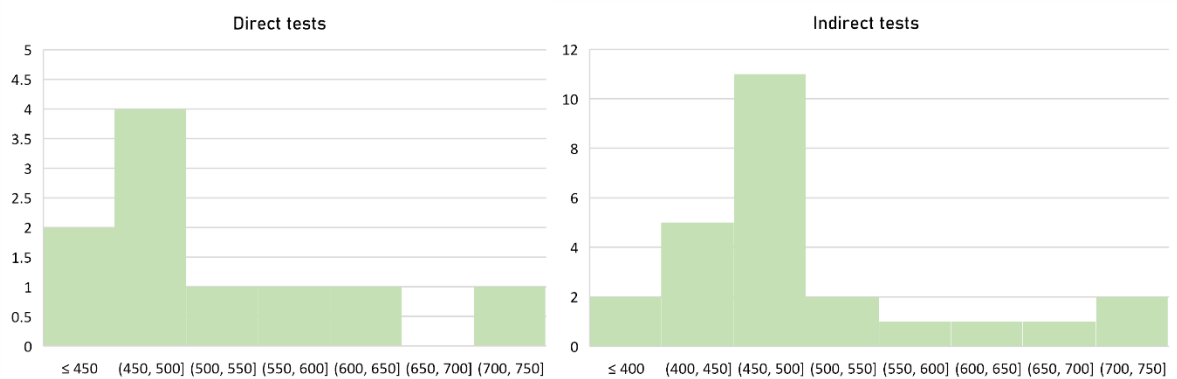


Figure 7. Frequency distribution after eliminating the three outlier results.

Specimens I, II, III and IV were subjected to the elastic wave characterisation as a prior stage before the compressive strength tests. The results of this characterisation (Table 5) together with the modulus of elasticity and Poisson ratios reported in Section 3.2 allowed to establish comparisons between these specimens and the materials tested in situ. This discussion is extensively reported in section 3.3. Nevertheless, the mean velocities obtained for samples I, II, III and IV are within the intervals observed during the on-site testing campaign.

Specimen	Mean velocity v_p $\left[\frac{m}{s}\right]$	Density ρ $\left[\frac{kg}{m^3}\right]$
I	688.67	1356.43
II	701.67	1230.61

III	661.67	1433.83
IV	680.33	1277.21
Mean	683.08	1324.52

Table 5. Elastic wave propagation velocities for specimens I, II, III and IV.

3.2 Compressive strength tests

As mentioned earlier, Specimens A, B and C were tested with a single load-controlled ramp at a rate of 5 kN/min. Results are summarised in Table 6. It is convenient to recall that this experiment was aimed at establishing a reasonable interval for setting the subsequent tests and is not conclusive in representing the overall mechanical performance of the samples.

Table 6. Results obtained for the compressive tests on specimens A, B and C.

Specimen	Max. compressive strength [MPa]	Strain at max. comp. strength [mm/mm]	E [MPa]
A	0.47	0.064	7.34
B	0.42	0.058	7.24
C	0.67	0.063	10.63
Mean	0.52		8.40

The behaviour of all the specimens was quite similar in the elastic range, although specimen C reached a significantly higher compressive strength (Figure 8). The behaviour observed after the limit of the elastic region must not be interpreted as a plastic region of the curve but as a softening-alike phenomenon associated with the loss of material. It was observed that the failure mode was similar for all samples, with the detachment of the external layers of the specimens resulting in a sudden loss of section (see Figure 9). This phenomenon was somehow expected since the external layers of the samples are less constrained than the core.

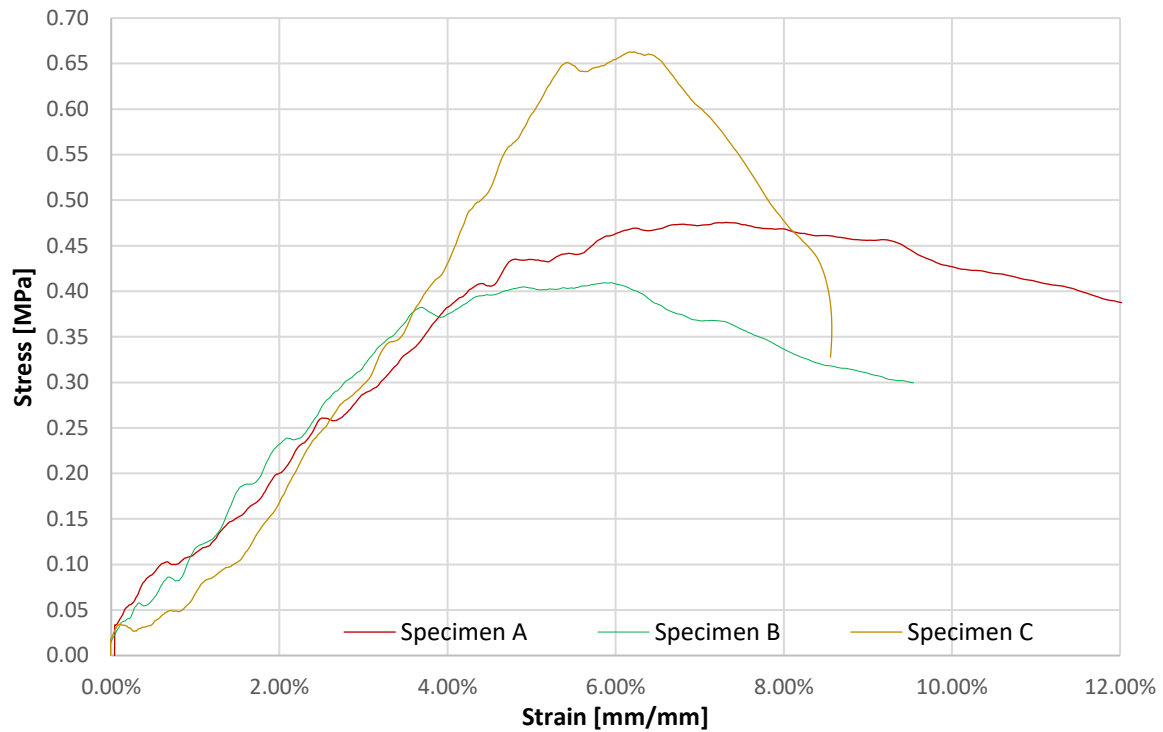


Figure 8. Strain/stress curves for specimens A, B and C.



Figure 9. Examples of the failure mode of samples A, B and C, with the detachment of the external layers of material.

The experiments on specimens I, II, III and IV were conducted with the support of OptoTrack-based strain gauges. The evaluation of strains in the X and Y directions allowed for the estimation of the Poisson's ratio for each specimen. Overall, the strain behaviour of all specimens was consistent and similar, although the differences in the reached maximum stress. The stress/strain curves, displayed in Figure 10, show similar progressive deformations for all samples. The maximum stresses, strains and mean Poisson's ratio are reported in Table 7.

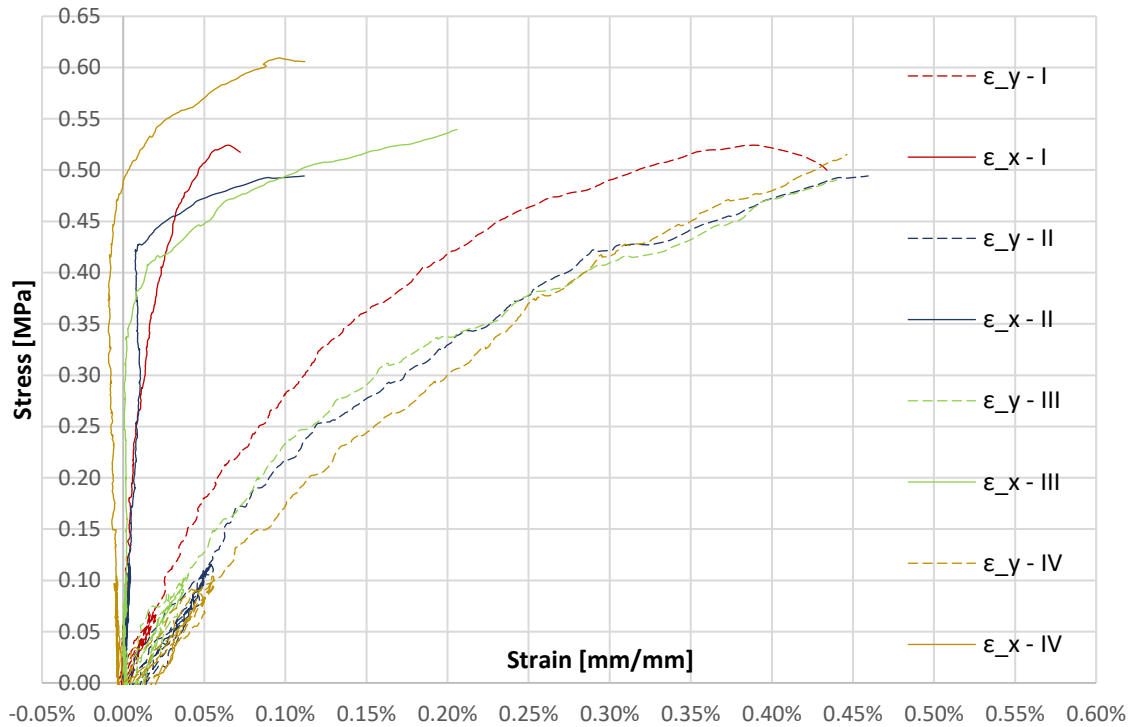


Figure 10. Stress/strain curves for specimens I, II, III and IV.

Table 7. Maximum stresses and strains, density, elasticity modulus and Poisson's ratio per specimen.

Specimen	Stress [MPa]	Strains in X and Y directions		Density [kg/m ³]	Elasticity Modulus E [MPa]	Poisson's Ratio ν
		ϵ_y	ϵ_x			
I	0.51	0.35%	0.05%	1356.43	145.78	0.15
II	0.43	0.31%	0.01%	1230.61	135.94	0.03
III	0.33	0.19%	0.00%	1433.83	173.18	0.01
IV	0.48	0.40%	0.00%	1277.21	119.35	0.00
Mean	0.44	0.32%	0.02%	1333.56	143.56	0.05

The hysteretic curves obtained during the load/unload cycles show that, despite a certain variability in the elastic behaviour, there is a consistent elastic recovery. This can be understood as a sign of the good condition of the specimens.

3.3 Analysis and Discussion

In Cuitiño, Rotondaro and Esteves (2020), the authors assess a series of experiences worldwide and report a wide variability of the compressive strength of this material, in a range of 0.3 and 2.06 MPa. This very significant range of value results, among other possible reasons, from the very different processes and proportions used in the fabrication of adobe. Even if narrowed down to Mexican references only, the wide range of values found in the literature is still significant. Sánchez, Alonso and Bedolla (2021) found mean values of 0.39 MPa. Arroyo Matus, Sánchez Tizapa and Catalán Quiroz (2013) report intervals from 0.59 up to 1.46 MPa from typical constructions in the south and centre of Mexico. Sanchez-Calvillo *et al.* (2020) reported mean values of 0.52 MPa for materials obtained from typical buildings in the state of Morelos. Contrastingly, Catalán Quiroz *et al.* (2019) reported mean values of 1.2 MPa for specimens produced in a laboratory. The values obtained during this experimental campaign seem close to the lower boundaries of the values found in the literature, close to 0.45 MPa. It is convenient to remember that the density of the materials herein presented is also lower than most of the typical values found in the literature.

It is important to bear in mind that the materials tested in the experiments reported herein were collected from seismic-damaged structures and after long-term storage (ca. five years) in uncontrolled outdoor conditions. For these reasons, the mechanical performance of these samples is expected to be lower than undamaged and well-preserved materials. Furthermore, it was not possible to dry the specimens under controlled conditions before testing due to the unavailability of proper equipment when this work was performed. Despite this limitation, and given that all the samples were collected, stored and tested together, it is reasonable to assume that the conditions among the samples are still comparable and equivalent.

Given the assumption of isotropy for this material (i.e., randomly oriented grains in which mechanical properties are not dependent on the macroscopic direction), Hooke's law is considered valid for correlating the velocity of propagation of a longitudinal elastic p-wave v_p as a function of the material density ρ , elastic dynamic modulus E_D and Poisson's ratio ν (Makoond, Pelà and Molins, 2019), as expressed in Eq. 1. This permits the obtention of the elastic dynamic modulus (Eq. 2).

$$v_p = \left(\frac{E_D(1 - \nu)}{\rho(1 + \nu)(1 - 2\nu)} \right)^{\frac{1}{2}} \quad (1)$$

$$E_D = \frac{v_p^2(\rho(1 + \nu)(1 - 2\nu))}{1 - \nu} \quad (2)$$

Since the ultrasonic elastic wave tests were also performed in these specimens, it was possible to obtain their dynamic modulus of elasticity and check if they were consistent with the static modulus of elasticity obtained in the laboratory tests (Table 8). Despite the relatively small number of samples, it was obtained a mean value of $E_d \cong 4.23E$. This proportion would be useful for contextualising boundaries for the modulus of elasticity of the materials tested in the ultrasonic wave propagation campaign.

Table 8. Summary of the elastic wave propagation velocity and modulus of elasticity per specimen

Specimen	Mean velocity v_p $\left[\frac{m}{s}\right]$	Density ρ $\left[\frac{kg}{m^3}\right]$	E [MPa]	E_D [MPa]	E_D/E
I	688.67	1356.43	145.78	607.00	4.16
II	701.67	1230.61	135.94	604.68	4.45
III	661.67	1433.83	173.18	627.64	3.62
IV	680.33	1277.21	119.35	591.15	4.95
Mean	683.08	1324.52	143.56	607.62	4.23

It is worth noting that the mean velocity $v_p = 683.08$ m/s obtained for specimens I, II, III and IV is comparable to the mean value of $v_p = 703.96$ m/s obtained for direct testing in the field campaign of Tepoztlán. This similarity suggests that the adobe pieces tested in the laboratory are representative of typical houses in Tepoztlán. However, this assumption is limited due to the small number of samples tested in the laboratory and the relatively low variability of velocities for each specimen.

These values obtained for the dynamic elastic modulus were compared to the ones obtained during the experimental laboratory campaign. According to the existing literature for Mexican adobe (Lacouture, L., Bernal, C., Ortiz, J. and Valencia, 2007), a Poisson ratio $\nu = 0.3$ is appropriate for this material. However, a value $\nu = 0.05$ was used to obtain the elastic dynamic modulus based on values found during the compressive tests (refer to Table 7). The values in Table 10 show a proportional

consistency between the direct p-wave tests on specimens I, II, III and IV and the set of direct tests conducted in situ.

Table 9. Mean dynamic modulus of elasticity per type of test.

Type		Mean velocity v_p	Standard deviation	E_D [MPa]
Direct	0	703.96	258.55	651.66
Direct	1	493.33	-	320.04
Direct	2	437.00	10.84	251.13
Indirect	0	507.01	90.60	338.04
Indirect	1	516.22	88.76	350.43
Indirect	2	394.50	1.65	204.65

Yet limited because of the variations found in the field campaign, the experimental results suggest a modulus of elasticity value of about 143 MPa and compressive strengths in the order of 0.45 MPa. The comparison provided in Table 10 is essential to conclude about the representativeness of the materials tested in the laboratory with respect to the typical adobe units found in the field ultrasonic testing campaign.

Table 10. Comparative between the mechanical characterisation performed through laboratory tests and a potential extrapolation based on the p-wave velocity tests in situ.

	Mean velocity v_p	Coefficient of Variation	Poisson Ratio ν	E [MPa]	E_D [MPa]	$\frac{E_D}{E}$
Lab*	683.08	0.025	0.05	143.56	607.62	4.23
Field*	703.96	0.367	0.05**	131.74**	557.28	4.23**
*Lab refers to mean values experimentally obtained for specimens I, II, III and IV, while Field refers to values experimentally obtained from ultrasonic p-wave tests in situ						
** Values obtained by extrapolating the Poisson's and E_D/E ratio experimentally obtained.						

It is worth noting that the properties of adobe walls as a mortar and unit composite cannot be directly associated with the mechanical properties of the adobe units. This is demonstrated by the significant differences in the p-wave transmission velocities obtained when testing single units versus measurements including mortar-unit interfaces. However, the number of measurements of this nature

was limited, despite the significant number of attempts made to enlarge this dataset of measurements (all unsuccessful, possibly due to internal discontinuities in the wall, which would be less likely in a wall with good quality and no damages).

A further necessary remark is related to the water content of the materials during the ultrasonic and laboratory test campaigns. Given some logistic limitations, it was impossible to assess the tested samples' water content. Nevertheless, it is possible to assume that the water content of the samples for compressive tests was similar to that of the materials tested during the field works. Furthermore, the sample collection and ultrasonic tests were performed at the end of August, i.e., in the middle of the rainy season for this region. A working hypothesis is that since the Puebla-Morelos earthquake occurred on 19th September 2017, it is reasonable to admit that the water content of materials was not drastically different.

4. Conclusions

A series of ultrasonic tests were performed in several historical adobe constructions in the municipality of Tepoztlán (Morelos, México). Most of the intended tests permitted retrieving replicable measurements, demonstrating thus the suitability of performing these tests in adobe units. Nevertheless, some difficulties were found while trying to measure the wave velocity of propagation in contiguous adobe pieces, indicating a potential disruption in the mortar interface. The tests conducted for characterising the propagation velocity of the mortar/unit system are, therefore, not conclusive.

On the other hand, the materials gathered in situ permitted to conduct of a series of laboratory experiments to characterise the compressive strength and the elastic behaviour of the material. Three calibration tests were initially carried out by fractioning a piece into three smaller specimens. These experiments allowed us to roughly estimate a range of between 0.40 and 0.60 MPa for ultimate strength. This value was adopted for designing the experiments for the rest of the specimens.

The four specimens (I, II, III and IV) were tested, and the stress/strain behaviour was captured using infrared LEDs and two sets of cameras. The mechanical behaviour seemed to be coherent and consistent throughout the samples, permitting us to obtain reasonably similar values for the modulus

of elasticity and ultimate compressive strength. Furthermore, the availability of results for ultrasonic propagation velocity on these pieces permits the validation of the hypothesis of the representativeness of these materials in the context of those assessed during field works.

The application of three initial load cycles permitted observing a good elastic recovery of the adobe pieces, indicating that the tested materials did not have damages that condition the results of the ultimate compressive strength tests. It was possible to obtain both static and dynamic modulus of elasticity by establishing analytical calculus involving Poisson's ratio and the p-wave velocity of propagation. These values have been critical for supporting indicative hypothetical values for the materials found in situ, in the proximities of modulus of elasticity of 143 MPa and ultimate compressive strengths of 0.45 MPa. Nevertheless, the p-wave propagation velocities obtained in situ present a relatively large range of variability, which limits the extrapolations herein proposed.

It is impossible to determine if the mechanical properties reported in this work can be extrapolated to a normal distribution for subsequent analyses, namely related to establishing typical values within a certain confidence interval. However, the mechanical properties herein reported are consistent with some values reported in the literature.

Although the number of tests is still considered too small for drawing conclusive results, it is worth noting that the materials herein presented correspond to historical construction. The possibility of testing a more extensive set of specimens is heavily conditioned by the availability of materials and their state of conservation. Despite these experiments cannot be considered conclusive for large-scale characterisation purposes, they can be complementary to future experimental campaigns in similar architectural typologies.

Future works aimed to enhance the results and observations herein presented should desirably include, for instance, humidity, water absorption and composition tests (e.g., granulometry and/or organic composition tests).

Even if the inconclusive experimental campaigns are often underestimated, the exceptionality of testing historical materials and the challenges faced while acquiring samples in certain environments are certainly reasons for considering the relevance and value of these observations.

Acknowledgements.

This work had the valuable help of Prof. Natalia García Gómez (Universidad Autónoma del Estado de Morelos), Eng. Víctor Hugo Torres Romero, M. Eng. Cyprien Lubin, Eng. Alexis Brito Sánchez and Tech. Arturo Fuerte (Universidad Nacional Autónoma de México).

The field campaigns in the State of Morelos were financed by the Instituto de Ingeniería – Universidad Nacional Autónoma de México (Institute of Engineering – National Autonomous University of Mexico) through the project R562.

This work was partly financed by FCT / MCTES through national funds (PIDDAC) under the R&D Unit Institute for Sustainability and Innovation in Structural Engineering (ISISE), under reference UIDB / 04029/2020. This work is financed by national funds through FCT - Foundation for Science and Technology, under grant agreement PD/BD/150385/2019 attributed to the 1st author.

References

- Archundia-Aranda, H. I. (2020) 'Seismic Damage at the State of Morelos (Mexico) due to September 19/2017 Earthquake', in *The 17th World Conference on Earthquake Engineering*. Sendai.
- Arroyo Matus, R., Sánchez Tizapa, S. and Catalán Quiroz, P. (2013) 'Caracterización experimental de las propiedades mecánicas de la mampostería de adobe del sur de México Characterization of the mechanical properties of southern Mexico 's adobe masonry', *Ingeniería*, 17(3), pp. 167–177. Available at: <http://www.redalyc.org/articulo.oa?id=46730914001%0D>.
- Catalán Quiroz, P. *et al.* (2019) 'Obtención de las propiedades mecánicas de la mampostería de adobe mediante ensayos de laboratorio', *Acta Universitaria*, 29, pp. 1–13. doi: 10.15174/au.2019.1861.
- CEMEX (2013) *Manual del constructor*. CEMEX, *Manual del Constructor*. CEMEX. Edited by CEMEX. Available at: [https://www.cemexmexico.com/Concretos/files/Manual del Constructor - Construcción General.pdf](https://www.cemexmexico.com/Concretos/files/Manual%20del%20Constructor%20-%20Construcci3n%20General.pdf).
- Chmutina, K., Jigyasu, R. and Okubo, T. (2020) 'Editorial for the special issue on “securing future of heritage by reducing risks and building resilience”', *Disaster Prevention and Management: An International Journal*, 29(1), pp. 1–9. doi: 10.1108/DPM-02-2020-397.
- Cuitiño, M., Rotondaro, R. and Esteves, A. (2020) 'Análisis comparativo de aspectos térmicos y resistencias mecánicas de los materiales y los elementos de la construcción con tierra TT -

Comparative analysis of thermal aspects and mechanical resistance of building materials and elements with earth', *Revista de Arquitectura*, 22(1), pp. 138–151. Available at: <https://bbibliograficas.ucc.edu.co/scholarly-journals/análisis-comparativo-de-aspectos-térmicos-y/docview/2476869316/se-2?accountid=44394>.

- Gavarini, C. (2001) 'Seismic risk in historical centers', *Soil Dynamics and Earthquake Engineering*, 21(5), pp. 459–466. doi: 10.1016/S0267-7261(01)00027-6.
- Godínez-Domínguez, E. A. *et al.* (2021) 'The September 7, 2017 Tehuantepec, Mexico, earthquake: Damage assessment in masonry structures for housing', *International Journal of Disaster Risk Reduction*, 56(February). doi: 10.1016/j.ijdr.2021.102123.
- Guerrero Baca, L. F. and Soria López, F. J. (2018) 'Traditional architecture and sustainable conservation', *Journal of Cultural Heritage Management and Sustainable Development*, 8(2), pp. 194–206. doi: 10.1108/JCHMSD-06-2017-0036.
- Jerónimo-Vargas, C. *et al.* (2022) 'Propuestas de adobe para viviendas vulnerables en el estado de Guerrero', *Pädi Boletín Científico de Ciencias Básicas e Ingenierías del ICBI*, 10(19), pp. 120–131. doi: 10.29057/icbi.v10i19.8247.
- Juárez, L., Caballero, T. and Morales, V. (2016) 'Ensayo de flexión lateral en muretes de adobe compactado reforzados con mallas de acero', *SÍSMICA 2004 - 6º Congresso Nacional de Sismologia e Engenharia Sísmica*, (February), pp. 544–555. Available at: http://www.hms.civil.uminho.pt/events/sismica2004/543-554_c13_Lidia_Argelia_Juarez_Ruiz_12p_.pdf.
- Lacouture, L., Bernal, C., Ortiz, J. and Valencia, D. (2007) 'Estudios de vulnerabilidad sísmica, rehabilitación y refuerzo de casas en adobe y tapia pisada', *Apuntes: Revista de Estudios sobre Patrimonio Cultural - Journal of Cultural Heritage Studies*, 20(2), pp. 20(2),286-303.
- Makoond, N., Pelà, L. and Molins, C. (2019) 'Dynamic elastic properties of brick masonry constituents', *Construction and Building Materials*, 199, pp. 756–770. doi: 10.1016/j.conbuildmat.2018.12.071.
- Ramírez Eudave, R. and Ferreira, T. M. (2021) 'On the potential of using the Mexican National Catalogue of Historical Monuments for assessing the seismic vulnerability of existing buildings: a proof-of-concept study', *Bulletin of Earthquake Engineering*, 19(12), pp. 4945–4978. doi: 10.1007/s10518-021-01154-5.
- Rojas, J., Ferrer, H. and S, J. C. (2009) 'Dynamic Behaviour of Adobe Masonry Houses in Central', in *11th Canadian Masonry Symposium*. Toronto.
- Ruiz Serrano, M. (2019) *Conformación de bloques de adobe con residuos de agave 'Angustifolia Haw'*.

Estrategia para el desarrollo Local sustentable en Santa María La Asunción, Zumpahuacán, Estado de México. Universidad Autónoma del Estado de México. Available at: <http://ri.uaemex.mx/handle/20.500.11799/105029>.

- Ruiz Sibaja, J. A. and Vidal Sánchez, F. (2015) 'Caracterización mecánica de piezas de adobe fabricado en la región de Tuxtla Gutiérrez', *Revista Espacio I+D Innovación más Desarrollo*, 4(7), pp. 130–154. doi: 10.31644/imasd.7.2015.a05.
- Sanchez-Calvillo, A. *et al.* (2020) 'Analysis and characterisation of adobe blocks in jojutla de Juárez, México. Seismic vulnerability and loss of the earthen architecture after the 2017 puebla earthquake', *International Archives of the Photogrammetry, Remote Sensing and Spatial Information Sciences - ISPRS Archives*, 54(M–1), pp. 1133–1140. doi: 10.5194/isprs-archives-XLIV-M-1-2020-1133-2020.
- Sánchez, A., Alonso, E. and Bedolla, J. (2021) 'Point-Load Test Assesment as Study of Adobe Buildings Damaged after the 2017 Puebla Earthquake'. doi: 10.23967/sahc.2021.189.
- Sánchez Calvillo, A., Alonso Guzmán, E. M. and López Núñez, M. del C. (2021) 'Vulnerabilidad sísmica y la pérdida de la vivienda de adobe en Jojutla, Morelos, México, tras los sismos de 2017', *Vivienda y Comunidades Sustentables*, (10), pp. 9–29. doi: 10.32870/rvcs.v2i10.162.
- Tyrakowski, K. (2013) 'Adobe - Un Material De Construcción Tradicional Del Altiplano Mexicano: Resultados De Un Examen De Laboratorio', *Jahrbuch für Geschichte Lateinamerikas*, 20(1). doi: 10.7767/jbla.1983.20.1.165.
- Uhnák, A. (2018) 'A tourism program of government and its place in the process of preservation of cultural heritage on the example of "pueblos mágicos" in Mexico', *European Journal of Science and Theology*, 14(4), pp. 179–192.
- UNESCO (2016) 'The HUL Guidebook: Managing Heritage in Dynamic and Continually Changing Urban Environments', *The 15th World Conference of the League of Historical Cities*, (June), p. 59.
- United Nations (2015) 'General Assembly: Resolution Adopted by the General Assembly on 3 June 2015', *2015 Third UN World Conference on Disaster Risk Reduction (WCDRR)*, 08955(June), pp. 1–24.

433 **Appendix 1**

434 **Summary of ultrasonic wave pulse propagation velocity tests.**

Data processing software PL-Link Version 3.0.5.0

Device data Name Pundit

Serial Number UP01-004-0119

Software Version 3.0.11

Hardware Revision C1

Signal (ADC Values) Maximum 32767

Minimum -32768

Meas. Range 2 V

Step Size ~30.52 μ V

Probe gain: 500x

Pulse Voltage: 200V

PRF: 25 Hz

435

Building	Sample	Measurement	Velocity (m/s)	Thickness (m)	Type of measurement	Number of joints traversed	Mean Value (m/s)
1	1	a	699	0.34	Direct	0	713.33
1	1	b	710				
1	1	c	731				
1	2	a	843	0.34	Direct	0	821.00
1	2	b	810				
1	2	c	810				
2	1	a	418	0.16	Indirect	0	463.00
2	1	b	484				
2	1	c	487				
2	2	a	486	0.16	Indirect	0	489.67
2	2	b	487				
2	2	c	496				
3	1	a	425	0.25	Indirect	0	425.67
3	1	b	424				

Building	Sample	Measurement	Velocity (m/s)	Thickness (m)	Type of measurement	Number of joints traversed	Mean Value (m/s)
3	1	c	428				
3	2	a	487	0.16	Indirect	0	517.00
3	2	b	486				
3	2	c	578				
4	1	a	463	0.185	Indirect	0	458.33
4	1	b	456				
4	1	c	456				
4	2	a	485	0.16	Indirect	0	480.67
4	2	b	473				
4	2	c	484				
5	1	a	714	0.141	Indirect	0	706.00
5	1	b	701				
5	1	c	703				
5	2	a	709	0.18	Indirect	0	705.33
5	2	b	704				
5	2	c	703				
6	1	a	647	0.4	Direct	0	646.67
6	1	b	646				
6	1	c	647				
6	2	a	567	0.15	Indirect	0	566.33
6	2	b	566				
6	2	c	566				
7	1	a	1005	0.35	Direct	0	1005.33
7	1	b	1005				
7	1	c	1006				
7	2	a	1013	0.35	Direct	0	1009.00
7	2	b	1005				
7	2	c	1009				
7	3	a	1236	0.35	Direct	0	1238.00
7	3	b	1244				
7	3	c	1234				
8	1	a	502	0.225	Direct	0	497.33

Building	Sample	Measurement	Velocity (m/s)	Thickness (m)	Type of measurement	Number of joints traversed	Mean Value (m/s)
8	1	b	497				
8	1	c	493				
9	1	a	467	0.17	Indirect	0	470.33
9	1	b	467				
9	1	c	477				
9	2	a	443	0.15	Indirect	0	443.00
9	2	b	443				
9	2	c	443				
9	3	a	671	0.17	Indirect	0	671.00
9	3	b	671				
9	3	c	671				
10	1	a	477	0.17	Direct	0	479.00
10	1	b	481				
10	1	c	472				
10	2	a	563	0.242	Direct	0	560.67
10	2	b	555				
10	2	c	564				
10	3	a	522	0.242	Direct	0	518.33
10	3	b	519				
10	3	c	514				
10	4	a	504	0.242	Direct	0	484.00
10	4	b	458				
10	4	c	490				
10	5	a	456	0.2	Indirect	0	456.00
10	5	b	456				
10	5	c	456				
10	6	a	411	0.25	Indirect	0	411.25
10	6	b	410				
10	6	c	410				
10	6	d	414				
10	7	a	498	0.13	Direct	1	493.33
10	7	b	491				

Building	Sample	Measurement	Velocity (m/s)	Thickness (m)	Type of measurement	Number of joints traversed	Mean Value (m/s)
10	7	c	491				
10	8	a	430	0.24	Direct	2	429.33
10	8	b	429				
10	8	c	429				
10	9	a	447	0.25	Direct	2	444.67
10	9	b	441				
10	9	c	446				
10	10	a	477	0.24	Direct	0	477.00
10	10	b	477				
10	10	c	477				
11	1	a	506	0.13	Indirect	0	505.00
11	1	b	506				
11	1	c	503				
11	2	a	615	0.14	Indirect	1	615.67
11	2	b	615				
11	2	c	617				
11	3	a	379	0.28	Indirect	2	393.33
11	3	b	400				
11	3	c	401				
12	1	a	461	0.16	Indirect	0	460.67
12	1	b	461				
12	1	c	460				
12	2	a	482	0.155	Indirect	0	481.33
12	2	b	481				
12	2	c	481				
12	3	a	449	0.15	Indirect	1	445.00
12	3	b	443				
12	3	c	443				
12	4	a	396	0.27	Indirect	2	395.67
12	4	b	395				
12	4	c	396				
13	1	a	494	0.15	Indirect	0	494.33

Building	Sample	Measurement	Velocity (m/s)	Thickness (m)	Type of measurement	Number of joints traversed	Mean Value (m/s)
13	1	b	495				
13	1	c	494				
13	2	a	427	0.2	Indirect	0	428.33
13	2	b	429				
13	2	c	429				
13	3	a	481	0.16	Indirect	1	488.00
13	3	b	491				
13	3	c	492				

436

437